Ionic liquid-tethered nanoparticle suspensions: A novel class of Ionogels

Journal:	*Chemistry of Materials*
Manuscript ID:	cm-2012-00424v.R1
Manuscript Type:	Article
Date Submitted by the Author:	n/a
Complete List of Authors:	Archer, Lynden; Cornell Univeristy, Dept of Chemical & Biomolecular Engineering Moganty, Surya Srivastava, Samanvaya Lu, Yingying; Cornell University, Schafer, Jennifer; Cornell University, Rizvi, Salmaan; Cornell University,

Manuscript for submission to *Chemistry of Materials,* March 2012

Ionic liquid-tethered nanoparticle suspensions: A novel class of Ionogels**

*Surya S. Moganty, Samanvaya Srivastava, Yingying Lu, Jennifer L. Schaefer, Salmaan A. Rizvi, and Lynden A. Archer**

* Prof. L.A. Archer, Dr. S. Moganty, S. Srivastava, Y.Y. Lu, J.L. Schafer, S.A. Rizvi School of Chemical and Biomolecular Engineering, Cornell University, Ithaca, NY 14853-5201 Email: laa25@cornell.edu

** This work was supported by Award No. KUS-C1-018-02, made by King Abdullah University of Science and Technology (KAUST), and by the National Science Foundation, Award No. DMR-1006323. JS acknowledges support from a National Science Foundation Energy & Sustainability IGERT fellowship program at Cornell.

Abstract

We report a novel class of silica ionogels created by dispersing silica nanoparticles densely grafted with the ionic liquid 1-trimethoxysilyl propyl-3-methyl-imidazolium bis(trifluoromethylsulfonyl) imide (SpmImTSFI) in a 1-butyl-3-methyl-pyrrolidinium bis(trifluoromethylsulfonyl) imide (BmpyrTFSI) IL host. We find that over the entire range of nanoparticle volume fractions studied the systems exist as stable suspensions of SiO_2-SpmImTFSI in the BmpyrTFSI host. Remarkably, we also find that addition of even minute quantities of SiO_2-SpmImTFSI to the BmpyrTFSI IL suppresses crystallization of the host. The resulting disordered hybrid fluids exhibit liquid-like transport properties over a vastly extended temperature range; they open the way for facile synthesis of ionic liquids with extended operating temperature windows. These observations are explained in terms of ionic coupling of the nanoparticle-tethered and free TFSI anions, which is thought to suppress crystallization of BmpyrTFSI.

Key Words: Ionic-liquid; Electrolytes; Nanoparticles; Crystallization; Tethered molecules

Introduction

Ionic Liquids (ILs) are organic salts having melting points below the boiling point of water. They generally consist of a bulky cation and anion. The large cation size allows for delocalization and screening of charges, resulting in a reduction in the lattice energy and thereby the melting point or glass transition temperature. ILs have received considerable recent attention as novel solvents for chemical synthesis and as electrolytes for electrochemical systems due to their many attractive properties, including ultralow vapor pressure, high dielectric constant, thermal stability, and redox robustness.[1-5] Recently, synthesis and stabilization of inorganic nanoparticles in ILs have been extensively studied.[6-10] Although the use of ILs as solvents for preparation, stabilization and functionalization of nanomaterials is only at an infancy stage, the versatility of IL properties are broadly understood to offer attractive possibilities for nanomaterials tailored for particular applications.[11,12]

A subclass of hybrid materials termed ionogels or ion gels, formed by infusing ILs in a solid or solid-like phase, has been emerging as novel materials for a variety of applications, such as supported catalysis, solid electrolytes, and drug delivery.[13] Different solid supports have been used to form ionogels: carbon nanotubes[14,15], polymers[16-18], gelators[19-20], silica nanoparticles[21] and other metal/metal oxide nanomaterials[12,22]. This field is expected to grow rapidly as opportunities the host and IL guest components of the hybrids offer for controlling properties are realized. Furthermore, by adjusting the interactions between the IL and its host, task specific or *smart* ionogels can be envisioned.

This paper reports on the thermal and mechanical properties of ionogels created by dispersing IL-tethered nanoparticles in an IL host. In particular, we study dispersions of 1-trimethoxysilyl propyl-3-methyl-imidazolium bis(trifluoromethylsulfonyl) imide tethered SiO_2 (SiO_2-SpmImTFSI) nanoparticles in 1-butyl-3-methyl-pyrrolidinium bis(trifluoromethyl sulfonyl) imide (BmpyrTFSI) and find that addition of the SiO_2-SpmImTFSI particles dramatically alter both the thermal and mechanical properties of their host at low and high particle loadings. Addition of as little as 0.1 wt% SiO_2-SpmImTFSI nanoparticles produces measurable changes in the thermal properties of the BmpyrTFSI IL. And modest increases in concentration of nanoparticles transformed the IL from a plastic crystalline material into a simple liquid, with no evidence of a melting transition. Further increase in the nanoparticle concentration leads to enhancements in mechanical properties of the ionic liquid. Our findings appear to open the way for novel IL-nanoparticle hybrid electrolytes, which do not crystallize. Such materials offer exciting opportunities for applications in electrochemical storage and conversion devices.

The ionic liquid BmpyrTFSI has attracted significant interest both as a so-called *plastic crystalline* material[23,24] and as a low-volatility tunable solvent. It is currently under active consideration for asymmetric electric double-layer capacitors,[25] in electrodeposition,[26,27] and for electrosynthesis.[28] BmpyrTFSI has also received attention as a solvent for synthesis of lanthanide compounds,[29] as well as for complex separation processes and supercritical fluid extraction.[30-32] BmpyrTFSI is a dense (ρ = 1.4 g/cm^3) viscous (μ = 89 cP) liquid at room temperature.[33] Its intrinsic room-temperature ionic conductivity is not high, $\sigma = 3.8 \times 10^{-5}$ S cm^{-1}, but can be increased to an acceptable level for electrochemical energy storage applications by addition of an appropriate salt. For

example, a 0.5M solution of lithium bis(trifluoromethylsulfonyl) imide (LiTFSI) in BmpyrTFSI exibits an ionic conductivity of 8.7 x 10^{-5} S cm^{-1} at 30 ^{o}C.[34]

Howlett et al. reported that lithium metal electrodes cycled in a 0.5M LiTFSI/BmpyrTFSI electrolyte show no sign of dendrite formation at rates up to 1.0 A cm^{-2}.[35] BmpyrTFSI has also been reported to exhibit an attractive electrochemical stability window of up to 4.2V and 5.2V vs Fc/Fc^{+} at current densities of 1 mA cm^{-2} and 5 mA cm^{-2}, respectively.[33] Additionally, as with many ILs, the material exhibits negligible volatility and excellent thermal stability up to its degradation temperature of 583K.[33] The self-diffusion coefficients for the two constituent ions $Bmpyr^{+}$ and $TFSI^{-}$ have been reported by the same authors to be 2.5 x 10^{-7} cm^2 s^{-1} and 2.0 x 10^{-7} cm^2 s^{-1} at 32 ^{o}C and the ion transference numbers are 0.53 and 0.47, respectively.

Among the different classes of electrolytes, solid electrolytes have been studied extensively due to their inherent advantages in terms of safety and reliability.[36-37] ILs with solid-like mechanical properties and enhanced functionality are attractive because they are potentially useful for electrochemical conversion and storage devices with unusual form factors and enhanced safety.[38-39] Inorganic nanoparticles incorporated into ionogels have, for example, been investigated as electrolytes for dye sensitized solar cells.[40] Shimano et al. reported that incorporation of silica nanoparticles into IL provides a facile route towards solid-like mechanical properties and, under certain circumstances, produce minimal effect on IL transport properties such as ionic conductivity.[41] Recently we reported that hybrid, self-suspended IL's created by tethering 1-trimethoxysilyl-undocyl-3-methylimidazolium bis(trifluoromethylsulfonyl) imide to ZrO_2 nanostructures maintain most of the attractive features of the untethered IL, including thermal stability,

ionic conductivity and electrochemical stability, but exhibit substantially improved mechanical properties and lithium ion transference numbers.[42] An important trait of these self-suspended hybrid ILs is their soft-glassy flow behavior, which causes them to flow and deform like liquids when subjected to high stresses, but to regain solid-like consistency when the stress is removed.[42-43] In a series of articles, Watanabe and co-workers have also reported systematic studies of colloidal stability, ionic transport and viscoelastic properties of nanocomposites based on silica nanoparticles dispersed in ILs.[21,44] The authors showed that the surface chemistry and volume fraction of the particles can be used to control the stability and flow properties of the nanocomposites.

The IL/SiO_2-SpmImTFSI dispersions used in the current study were created, by blending BmpyrTFSI and SiO_2-SpmImTFSI in acetone. Removal of the acetone followed by rigorous drying of the materials yielded IL/SiO_2-SpmImTFSI dispersions with a range of SiO_2 loadings. Scheme 1 illustrates the procedure used for synthesizing SiO_2-SpmImTFSI. Figures 1(a) and 1(b) are, respectively, the H-NMR spectra for the untethered and silica-tethered 1-trimethoxysilyl propyl-3-methyl-imidazolium chloride (SpmImCl) precursor dissolved in dimethyl sulfoxide (DMSO) containing 0.03 vol% of tetramethylsilane (TMS) as an internal standard. With the exception of the two lines associated with the solvent DMSO and TMS, the NMR spectra of both materials are consistent with expected results for pure and particle-tethered ILs. In particular, the noticeably broader NMR lines evident by comparing Figures 1 (b) and 1(a) are consistent with expectations for the tethered imidazolium salt.

Results from dynamic light scattering (DLS) measurements, Fig. 2(a), shows that the hydrodynamic radius of the SiO_2-SpmImTFSI particles increases from 4.3 nm to 7.7 nm

after tethering the IL to SiO_2. The latter result is in agreement with conclusions from Transmission electron microscopy (TEM) measurements (Fig. 2(b)), which show that the SiO_2-SpmImTFSI particles disperse well in BmpyrTFSI and have an average radius of ca. 4.8 nm. The modest difference in the SiO_2 core size deduced from DLS from the unfunctionalized/bare particles and from TEM of the BmpyrTFSI/ SiO_2-SpmImTFSI are a result of two factors: (i) The slight enlargement of the core size produced by the silane coat at the IL-tethered particle surface; and (ii) The fact that the property measured by each of the two measurement techniques are sensitive to subtly different moments of the particle size distribution.

Characterization by thermal gravimetric analysis (Fig. 3) shows that the BmpyrTFSI, IL host, remains thermally stable up to temperatures around 450 ^{o}C (Fig. 3, inset) and that the SiO_2-SpmImTFSI remains stable up to temperatures about 25 ^{o}C higher. The enhanced stability of the tethered SpmImTFSI IL is also evident in the IL/SiO_2-SpmImTFSI dispersions containing a large-enough fraction of the tethered IL (see Fig. 3, inset), which show two degradation processes that correspond roughly to the two components in these blends, BmpyrTFSI and the SpmImTFSI tethered SiO_2 nanoparticles. The TGA trace for the SiO_2-SpmImTFSI further shows that the mass fraction of the inorganic component (w_{inorg}) is around 77%. Taking the density of the SiO_2 nanoparticles ρ_{SiO2} to be 2.2 g/cm^3 (i.e. the value for bulk SiO_2) and the average particle diameter a_{SiO2} to be 9.6 nm. (i.e. the estimate from TEM), the TGA data for SiO_2-SpmImTFSI indicates that there are close to 250 IL ligands tethered to each particle. This corresponds to a grafting density $\sum = N_A \frac{(1-w_{inorg})}{w_{inorg}} \frac{a_{SiO2}\rho_{SiO2}}{6M_{ligand}} \approx 0.8$ ligands/nm^2 and

a spacing of around 0.2 nm between the IL ligands tethered to the SiO_2 nanoparticle particle surface. Here M_{ligand} and N_A are, respectively, the molecular weight of the tethered IL and Avogadro's number.

The main results of the communication are summarized in Figures 4(a) and 4(b). These figures report on thermal transitions in BmpyrTFSI IL, as well as for the BmpyrTFSI /SiO_2-SpmImTFSI dispersions, deduced from differential scanning calorimetry (DSC) measurements at a fixed temperature ramp rate of 5 ^oC/min. Fig. 4(a) shows that pure BmpyrTFSI IL manifests a glass transition at a temperature, $T_g \approx$ -87 ^oC, a crystallization transition at, $T_c \approx$ -60 ^oC, and a melting transition at a temperature $T_m \approx$ -18 ^oC. BmpyrTFSI also exhibits a metastable phase with melting temperature of -24 ^oC. The crystallization transition following T_g indicates that the as prepared material is in a supercooled state. All of the observed thermal transitions are in fair accord with literature results.[23-24]

Remarkably, Fig. 4(a) also shows that addition of as little as 0.1 wt% SiO_2-SpmImTFSI nanoparticles to BmpyrTFSI has a dramatic effect on both the crystallization and melting transitions, but no effect on the glass transition. Specifically, the figure shows that T_g for the BmpyrTFSI IL is unaffected by addition of SiO_2-SpmImTFSI, but that both the energy change due to crystallization from the supercooled state and from the melting transition are considerably reduced; the transition temperatures however remain more or less the same. At higher loadings of the SiO_2-SpmImTFSI nanostructures, the effect remains, but its magnitude is largely unaffected by the nanoparticle content. However, at 40wt% particle loading (Fig. 4(b)) both the crystallization and melting transitions

disappear, and the material exhibits only a glass transition temperature ($T_g \approx$ -85 ^oC), essentially the same as for the pure BmpyrTFSI.

Our observations have striking similarities to a recent report, which shows that room temperature blending of the salt LiTFSI, a solid, and SiO_2-SpmImTFSI nanostructures, also solid, yields a liquid with enhanced ionic conductivity and lithium transference number.[45] X-ray Diffraction analysis of the LiTFSI with and without the SiO_2-SpmImTFSI component, nicely show that the fluidity of the blends originate from the ability of the SiO_2-SpmImTFSI to disrupt crystallization of the salt. As an explanation for the effectiveness of the SiO_2-SpmImTFSI particles in suppressing crystallization of their IL host in the present case, we hypothesize that the common counterion (TFSI) effectively couples the nanopaticle-tethered IL cations (Im+) and free Bmpyr+ ions, which hinders crystallization of the BmpyrTFSI IL.

The ionic radius of the bis(trifluoromethanesulfonyl)imide (TFSI) anion has been estimated using hole theory to be 0.36 nm,[46] and the Van-der-Waals radii of TFSI has been reported to be 0.33 nm.[46-47] Based on the ligand spacing of 0.2 nm calculated earlier, this implies that there is simply not enough space on the particle surface for each TFSI ion to be associated with a single tethered imidazolium ligand. Thus, it can be argued that the seeds for non-specific coupling between the free BmpyrTFSI and particle-tethered SpmImTFSI are already present at the particle surface; perhaps explaining why even a small amount of particles produces the rather large effect on the melting transition noted in Fig. 4(a).

Electrostatic coupling between the tethered SpmImTFSI and untethered BmpyrTFSI should also have an effect on viscous properties of BmpyrTFSI. Fig. 5(a) shows that the viscosity of the BmpyrTFSI /SiO_2-SpmImTFSI dispersions increase by more than three orders of magnitude over the same range of SiO_2 nanoparticle concentrations where the most significant changes in melting behavior are seen, but largely remain simple Newtonian fluids over the same range of nanoparticle concentrations where the most notable effects on thermal properties are observed. Significantly, even for the highest particle loadings a Newtonian regime can be found for all of the materials. The existence of a Newtonian flow regime in a nanoparticle suspension indicates that the system is able to reach equilibrium,[48] a feature that is normally not observed for suspensions in which the particulate phase is unstable and able to aggregate. Reports by Watanabe et al. show that addition of as little as 2-3wt% of silica nanoparticles in EmImTFSI and EmImBF_4 ILs leads to pronounced shear thinning due to flocculation and agglomeration of the particles.[21,44]

Additional evidence for the colloidal stability of the suspensions is seen in Fig. 5(b), which reports the frequency-dependent dynamic elastic modulus, G' (filled symbols), and viscous loss modulus G'' (unfilled symbols) for BmpyrTFSI /SiO_2-SpmImTFSI dispersions with very high particle loadings. The data shows that, but for the highest particle loading, $G'' > G'$ over the entire range of frequency studied, a feature that would not be seen in a suspension of aggregated nanoparticles even at 10-times lower particle loadings. We suspect that both the viscous and less shear sensitive behavior observed in the materials is a result of the improved dispersion of SiO_2 in the BmpyrTFSI host made possible by the imidazolium TFSI surface functionalization.

The relative viscosity, $\eta_r \equiv \eta_0 / \eta_s$, of a concentrated suspension of hard spheres has been related to the volume fraction of particles by the so-called Krieger-Dougherty formula,[48-49]

$$\eta_r = (1 - \frac{\phi}{\phi_{\max}})^{-[\eta]\phi_{\max}} \qquad (1)$$

Where, η_0 and η_s are the zero shear viscosity of the suspension and the suspending medium, respectively; ϕ and ϕ_{max} are the volume fraction of particles in suspension and the maximum volume fraction for close packing of the suspended phase; and $[\eta]$ is the intrinsic viscosity. By fitting *Eq.* (1) (continuous line) to the experimental data for the BmpyrTFSI IL/SiO_2-SpmImTFSI (Fig. 5(c)), we find $[\eta] = 20$ and ϕ_{max} = 0.63. While the value of $[\eta]$ is substantially different from expectations for a suspension of randomly arranged hard spheres, for which $[\eta]$ is 2.5, ϕ_{max} is close to the expected value of 0.64. It is known that the intrinsic viscosity of a suspension of sterically stabilized or charged spheres can be determined from knowledge of the hard-sphere intrinsic viscosity $[\eta]_{HS}$ using the formula, $[\eta] = [\eta]_{HS}(1 + \frac{\lambda}{a})^3$,[49] where a is the core particle radius and λ is a characteristic length scale (e.g. polymer brush height or Debye screening length), which defines the range of the interactions. Substituting the experimental values, we find $\lambda \approx a \approx 4.9\text{nm}$. This value is more than seven times the combined van der-Waals radius of Bmpyr (0.34 nm) and TFSI (0.33 nm). It is also substantially larger than the thickness of the tethered IL layer on the particles. The fact that the range of interactions in the IL is around seven molecular radii is consistent with the calculations of Ferdorov and Kornsyshev for the electrostatic double layer in ionic liquids near charged surfaces.[50] In

particular these authors found that the potential exhibits strong spatial oscillations consistent with the presence of multiple ionic layers that extend to distances many times the molecular size from the charged substrate. Such long-range interactions in ILs have also been noted in IL-nanotube dispersions, where local ordering of the IL phase is thought to produce cross-linking/entanglements between the nanotubes.[14]

In an effort to understand how interactions between SiO_2-SpmImTFSI nanoparticles and the BmpyrTFSI IL host might alter physical properties of the host, we performed Small angle X-ray scattering (SAXS) measurements [52-53] at 30°C. To maximize the photon flux, measurements employed a line collimated source for which the measured scattering intensity, $I_{\exp}(q)$, is related to that measured using point collimation, $I_o(q)$ by,

$$I_{\exp}(q) = \int_{-\infty}^{\infty} W_x(x) \int_{-\infty}^{-\infty} W_y(y) I_o(\sqrt{(q-y)^2 + x^2}\, dy dx \qquad (2)$$

where $W_x(x)$ and $W_y(y)$ are the slit length and slit width profiles, respectively, and q is the scattering wave vector. Figure 6(a) are the small-angle $I_{\exp}(q)$ for I BmpyrTFSI /SiO_2-SpmImTFSI dispersions at both low and high particle loadings. At small q and low nanoparticle loadings, the suspensions show typical dilute suspension scattering behavior with $I(q) \sim q^2$. At higher SiO_2 weight fractions the scattered intensity at any q is nearly proportional to the particle loading, again as expected. What is unexpected is the shape of the particle pair distribution function, PDDF (Fig. 6(b)).

$$p(r) = \frac{r^2}{2\pi} \int_0^{\infty} I_o(q) \frac{\sin(qr)}{qr} dq \qquad (3)$$

Specifically, based on the analyses using DLS (Fig. 2(1)), TEM (Fig. 2(b)) and rheology (Fig. 5) measurements, it appears that the SiO_2-SpmImTFSI particles are stable against

agglomeration and are homogeneously dispersed in the BmpyrTFSI IL host. The shape of $p(r)$ seen in Fig. 6(b) tells a more complex story. Namely that there is substantial probability of finding scatters at all distances relative to a selected particle located at the origin, and that the probability is moderately larger at radial distances that are integer multiples of the hydrodynamic size of the SiO_2-SpmImTFSI nanoparticles. This finding implies that the particle positions in the BmpyrTFSI IL/SiO_2-SpmImTFSI dispersions are correlated over distances comparable to the particle size. It is also consistent with the intrinsic viscosity data, which indicate that the particles interact over distances comparable to the SiO_2 core particle size.

In summary, we report on the synthesis of SiO_2 nanoparticles densely functionalized with an imidazolium based ionic liquid and investigate the thermophysical properties in blends with the ionic liquid BmpyrTFSI. We find that crystallization of the BmpyrTFSI IL host can be partially suppressed by addition of minute amounts of the particle-tethered IL, and that crystallization of the host is completely suppressed in blends with nanoparticle loadings above a moderate threshold value. Using a combination of physical characterization methods, we explore the source of the observations and hypothesize that SiO_2-SpmImTFSI prevents crystallization of the un-tethered BmpyrTFSI IL host by coupling with the host via their common counterion, TFSI. The results reported in this communication show that ionic-liquid functionalized nanoparticles can be used in previously unexplored ways to manipulate the melting transition of ionic liquids.

Experimental Section

Synthesis of IL tethered silica nanoparticles

All chemicals used in the study were purchased from Sigma Aldrich and used as received. The approach used for synthesizing SiO_2-SpmImTFSI nanoparticles is illustrated in Scheme 1. Briefly, the ionic liquid precursor 1-trimethoxysilyl-propyl-3-methyl imidazolium chloride was first synthesized according to a previously reported procedure.[42,51] The purity of the resultant IL was verified by H-NMR Spectroscopy (see Fig. 1(a)). The as prepared 1-trimethoxysilylpropyl-3-methyl-imidazolium chloride IL was tethered to silica nanaoparticles in a simple one-pot synthesis. In a typical reaction, colloidal silica nanoparticles (SM-30 from Aldrich) were first diluted to 2 wt% in deionized water, and a 1.5 times excess of 1-trimethoxysilylpropyl-3-methyl-imidazolium chloride IL added slowly with continuous stirring for 12 hrs at 100 ^{o}C. After 12 hrs, ethanol was added and the IL functionalized silica nanoparticles separated by centrifugation. The ethanol washing was repeated for at least three times and the silica particles were dried by lyophilization/freeze drying. The purity of the resultant SiO_2-SpmImCl was confirmed using proton NMR spectroscopy (Fig. 1(b)).

To convert the SiO_2-SpmImCl to the desired SiO_2-SpmImTFSI, anion exchange was performed on the IL-tethered silica nanoparticles using a simple procedure. In a typical anion exchange reaction, 10 g SiO_2-SpmImCl were dispersed in 300 ml DI water; the Cl anion IL functionalized silica particles are hydrophilic and formed a clear dispersion in water. To this clear mixture 8g of lithium bis(trifluoromethylsulfonyl)imide (LiTFSI) salt dissolved in 50 ml DI water was added with stirring. Immediately following addition, the silica particles separated from the water phase and settle to the bottom of vessel due to

the hydrophobic nature of the TFSI anion exchanged particles. Then resultant SiO_2-SpmImTFSI nanoparticles were centrifuged, washed with DI water, dried and re-dispersed in acetone. Silica particles with partially exchanged Cl anions settle out of acetone and were discarded. The purified SiO_2-SpmImTFSI nanoparticles were dried and used for making dispersions in the BmpyrTFSI IL. Analysis of the SiO_2 particle size and size-distribution before and after functionalization with imidazolium IL was performed using light scattering in water and acetone, respectively, as well as by electron microscopy and thermal gravimetric analysis (TGA).

2. Thermal Properties

Differential scanning calorimetry (DSC) was used to characterize thermal transitions in BmpyrTFSI/SiO_2-SpmImTFSI blends as a function of the inorganic particle loading. Measurements were performed using a TA Instruments DSC Q2000 at a scan rate of 5 ^oC per minute in a Nitrogen (N_2) environment.

3. Rheological Measurements

Rheology measurements was performed using a stress controlled Anton Paar MCR 501 mechanical rheometer with 25 mm cone and plate fixtures (gap angle 4^o). Steady and oscillatory shear flow deformations were used to investigate the viscous flow and viscoelastic properties of the materials.

4. Small Angle X-Ray Scattering Measurements

Small angle X-ray scattering (SAXS) measurements were performed on an in-house Anton Paar SAXSess mc^2 scattering system. The instrument has a sealed tube line collimated X-ray source and imaging plate detectors. Custom made Quartz capillary sample holders were used and the temperature was maintained at 30^oC using Peltier

temperature controller. The GIFT software program was used to determine $I_o(q)$ by approximating $p(r)$ with a set of cubic-B-splines. Once $I_o(q)$ is known, $I_{exp}(q)$ can be computed via *Eq* 2 using the known slit length and width profiles.

References

[1] Welton, T. *Chem. Rev*. **1999**, 99, 2071-2084; Wasserscheid, P.; Welton, T. *Ionic liquids in Synthesis,* Wiley-VCH, Weinheim, **2008**.

[2] Bonhote, P.; Dias, A.P.; Papageorgiou, N.; Kalyanasundaram, K.; Gratzel, M. *Inorg. Chem.* **1996**, 35, 1168-1178; Blanchard, L.A.; Hancu, D.E.; Beckman, J.; Brennecke, J.F. *Nature* **1999**, 399, 28-29.

[3] Giernoth, R. *Angew. Chem. Int. Ed.* **2010**, 49, 5608-5609; Hapiot, P.; Lagrost, C. *Chem. Rev.* **2008**, 108, 2238-2264.

[4] Ohno, H. *Eletrochemical Aspects of Ionic Liquids*, John Wiley & Sons, Hoboken, NJ, **2005**.

[5] Moganty, S.S.; Baltus, R.E.; Roy, D. *Chem. Phys. Lett.* **2009**, 483, 90-94; Moganty, S.S.; Baltus, R.E. *Ind. Eng. Chem. Res*. **2010,** 49, 5846-5853.

[6] Scheeren, C.W.; Machado, G.; Dupont, J.; Fichtner, P.F.P.; Texeira, S.R. *Inorg. Chem*. **2003,** 42, 4738-4742.

[7] Dupont, J.; Fonseca, G.S.; Umpierre, A.P.; Fichtner, P.F.P.; Texeira, S.R. *J. Am. Chem. Soc*. **2002**, 124, 4228-4229.

[8] Fonseca, G.S.; Machado, G.; Texeira, S.R.; Fecher, G.H.; Morias, J.; Travers, A.; Dupont, J. *J. Colloid Interface Sci.* **2006**, 301, 193-204.

[9] Cassol, C.C.; Umpierre, A.P.; Machado, G.; Wolke, S.I.; Dupont, J. *J. Am. Chem. Soc*. **2005**, 127, 3298-3299.

[10] Gelesky, M.A.; Chiaro, S.S.X.; Pavan, F.A.; dos Santos, J.H.Z.; Dupont, J. *Dalton Trans.* **2007**, 47, 5549-5553.

[11] Ma, Z; Yu, J.; Dai, S. *Adv. Mater*. **2010**, 22, 261-285.

[12] Dupont, J.; Scholten, J.D. *Chem. Soc. Rev*. **2010**, 39, 1780-1804; Neouze, M.-A. *J. Mater. Chem*. **2010**, 20, 9593-9607.

[13] Bideau, J.L.; Viau, L.; Vioux, A. *Chem. Soc. Rev*. **2011**, 40, 907-925; Valkenberg, M.H.; deCastro, C.; Holderich, W.H. *Green Chem*. **2002**, 4, 88-93.

[14] Fukushima, T.; Kosaka, A.; Ishimura,Y.; Yamatomo, T.; Takigawa, T.; Ishii, N.; Aida,T. *Science* **2003**, 300, 2072-2074.

[15] Fukushima, T.; Aida,T. *Chem. Eur. J.* **2007**, 13, 5048-5058.

[16] Susan, M.A.B.H.; Kaneko, T.; Noda, A.; Watanabe, M. *J. Am. Chem. Soc*. **2005**, 127, 4976-4983.

[17] Bruce, P.G.; Scrosati, B.; Tarascon, J.M. *Angew. Chem. Int. Ed.* **2008**, 47, 2930-2946.

[18] Lu, J.; Yan, F.; Texter, J. *Prog. Polym. Sci.* **2009**, 34, 431-448; Gayet, F.; Viau, L.; Leroux, F.; Monge, S.; Robin, J.-J.; Vioux, A. *J. Mater. Chem.* **2010**, 20, 9456-9462.

[19] Kubo, W.; Kambe, S.; Nakade, S.; Kitamura, T.; Hanabusa, K.; Wada, Y.; Yanagida, S. *J. Phys. Chem. B.* **2003**, 107, 4374-4381.

[20] Voss, B.A.; Bara, J.E.; Gin, D.L.; Noble, R.D. *Chem. Mater.* **2009,** 21, 3027-3029.

[21] Ueno, J.K.; Inaba, A.; Kondoh, M.; Watanabe, M. *Langmuir* **2008**, 24, 5253-5259; Ueno, J.K.; Inaba, A.; Sano, Y.; Kondoh, M.; Watanabe, M. *Chem. Comm.*

2009, 24, 3603-3605; Ueno, J.K.; Imaizumi, S.; Hata, K.; Watanabe, M. *Langmuir* **2009**, 25, 825-831.

[22] Kim, J.D.; Mori, T.; Kudo, T.; Homma, I. *Solid State Ionics* **2008**, 179, 1178-1181.

[23] MacFarlane, D. R.; Huang, J.; Forsyth, M. *Nature* **1999**, 402, 792-794.

[24] Anderson, W.A.; Passerini, S. *Chem. Mater.* **2004,** *16*, 2881-2885; MacFarlane, D.R.; Forsyth, M. *Adv. Mater.* **2001**, 13, 957-966.

[25] Lazzari, M.; Mastragostino, M.; Pandolfo, A.G.; Ruiz, V.; Soavi, F. *J. Electrochem. Soc.* **2011**, 158, A22-A25; Lazzari, M.; Soavi, F.; Mastragostino, M. *Fuel Cells* **2010**, 5, 840-847.

[26] Masud, J.; Alam, M.T.; Okajima, T.; Ohsaka, T. *Chem. Lett.* **2011**, 40, 252-254.

[27] Basile, A.; Bhatt, A.I.; O'Mullane, A.P.; Bhargava, S.K. *Electrochim. Acta* **2011**, 56, 2895-2905.

[28] Österholma, A.; Kvarnströmb, C.; Ivaska, A. *Electrochim. Acta* **2011**, 56, 1490-1497.

[29] Babai, A.; Mudring, A.-V. *Chem. Mater.* **2005**, 17, 6230-6238.

[30] Nebig, S.; Gmehling, J. *Fluid Phase Equilibria* **2011**, 302, 220-225; Nebig, S.; Liebert, V.; Gmehling, J. *Fluid Phase Equilibria* **2009***,* 277, 61-67.

[31] Pereiro, A.B.; Rodrıguez, A. *AIChE Journal* **2010**, 56, 381-386.

[32] Yim, J-H.; Song, H.N.; Yoo, K.-P.; Lim, J.S. *J. Chem. Eng. Data* **2011**, 56, 1197-1203.

[33] O'Mahony, A.M.; Silvester, D.S.; Aldous, L.; Hardacre, C.; Compton, R.G. *J. Chem. Eng. Data* **2008**, 53, 2884-2891.

[34] Stefan, C.S.; Lemordant, D.; Biensan, P.; Siret, C.; Claude-Montigny, B. *J Therm. Anal. Calorim.* **2010**, 102, 685-693.

[35] Howlett, P.C.; MacFarlane, D.R.; Hollenkamp, A.F. *Electrochem. Solid State Lett.* **2004**, 7, A97-A101.

[36] Torimoto, T.; Tsuda, T.; Okazaki, K.; Kuwabata, S. *Adv. Mater*. **2010**, 21, 1196-1221.

[37] Armand, M.; Endres, F.; MacFarlane, D.R.; Ohno, H.; Scrosati, B. *Nature Mater.* **2009**, 8, 621-629.

[38] Castiglione, F.; Ragg, E.; Mele, A.; Appetecchi, G.B.; Montanino, M.; Passerini, S. *J. Phys. Chem. Lett.* **2011**, 2, 153-157.

[39] Wang, P.; Zakeeruddin, S.M.; Comte, P.; Exnar, I.; Gratzel, M. *J. Am. Chem. Soc*. **2003**, 125, 1166-1167.

[40] Katakabe, T.; Kawano, R.; Watanabe, M. *Electrochem. Solid State Lett.* **2007,** 10, F23-F25.

[41] Shimano, S.; Zhou, H.; Honma, I. *Chem. Mater.* **2007**, 19, 5216-5221.

[42] Moganty, S.S.; Jayaprakash, N.; Nugent, J.L.; Shen, J.; Archer, L.A. *Angew. Chem. Int. Ed.* **2010**, 49, 9158-9161.

[43] Agarwal, P.; Qi, H.; Archer, L.A. *Nano. Lett.* **2010**, 10, 111-115; Agarwal, P; Srivastava, S.; Archer, L.A. *Phys. Rev. Lett*. 2011, **107**, 268302.

[44] Ueno, K.; Inaba, A.; Sano, Y.; Kondoh, M.; Watanabe, M. *J. Phys. Chem. B* **2010**, 114, 13095-13103.

[45] Lu, Y.; Moganty, S.S.; Schaefer, J.L.; Archer, L.A. *J. Mater. Chem.* **2012**, 22, 4066-4072.

[46] Abbott, A.T. *Chem. Phys. Chem.* **2004**, 5, 1242-1246.

[47] Ue, M.; Murakami, A.; Nakamura, S. *J. Electrochem. Soc.* **2002,** 149**,** A1572-A1577.

[48] Krieger, L.M.; Dougherty, T.J. *Trans. Soc. Rheol.* **1959**, 3, 137-152.

[49] R. G. Larson, *Structure and Rheology of Complex Fluids*, Oxford University Press, New York, **1998**.

[50] Fedorov, M.V.; Kornyshev, A.A. *Electrochim. Acta,* **2008**, 53, 6835-6840.

[51] S. S. Moganty, *PhD Thesis,* Clarkson University, **2009**.

[52] Litschauer, M.; Peterlik, H.; Neouze, M.A. *J. Phys. Chem. B*, **2009**, 113, 6547-6552.

[53] Litschauer, M.; Puchberger, M.; Peterlik, H.; Neouze, M.A. *J. Mater. Chem.*, **2010**, 20, 1269-1276.

Table of Contents Graphic

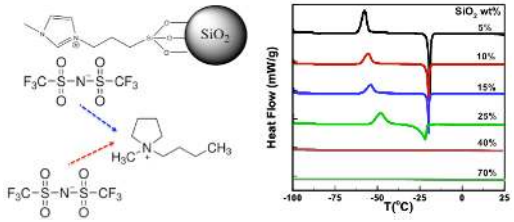

Summary: Ionogels created by blending ionic liquid-functionalized inorganic nanoparticles with an ionic liquid (IL) exhibit unusual thermal and physical properties. Even small amounts of IL-functionalized nanoparticles suppress crystallization of the IL host, and moderate amounts eliminate crystallization altogether. Our results suggest a new approach for tuning thermal properties IL electrolytes.

Figure Captions

Scheme 1. Schematic of procedure used for synthesizing SiO_2-SpmImTFSI nanoparticles.

Figure 1 (a) H-NMR spectrum of 1-trimethoxysilylpropyl-3-methyl-imidazolium chloride in DMSO; (b) H-NMR spectrum of SiO_2-SpmImCl in DMSO.

Figure 2. (a) Size-distribution of bare and SiO_2-SpmImTFSI nanostructures from dynamic light scattering measurements in water and acetone, respectively; (c) Transmission electron micrograph of BmpyrTFSI/SiO_2-SpmImTFSI.

Figure 3. Thermal gravimetric analysis of pure BmpyrTFSI, SiO_2-SpmImTFSI, and BmpyrTFSI/SiO_2-SpmImTFSI suspensions at three particle loadings. The inset is the differential weight loss for the materials as noted in the legend.

Figure 4. (a), (b) DSC thermograms of pure BmpyrTFSI and BmpyrTFSI/SiO_2-SpmImTFSI suspensions with increasing weight fraction of silica. Each curve is shifted successively by two units to enhance clarity of the graphic.

Figure 5. (a) Shear viscosity versus shear rate for BmpyrTFSI/SiO_2-SPMIMTFSI suspension with varying SiO_2 loadings; (b) Frequency-dependent dynamic storage, G' (filled symbols), and loss, G'' (unfilled symbols), modului for IL/SiO_2-IL suspensions; (c) Relative viscosity as a function of silica volume fraction for the BmpyrTFSI/SiO_2-SpmImTFSI suspensions. The fit is obtained using the K-D formula, *Eq.* 1 in the text.

Figure 6. (a) Scattering intensity as a function of wave vector for varying particle loading in the suspensions. The fits are obtained using GIFT software; (b) PDDF for BmpyrTFSI /SiO_2-SpmImTFSI suspensions as a function of inter-particle distance.

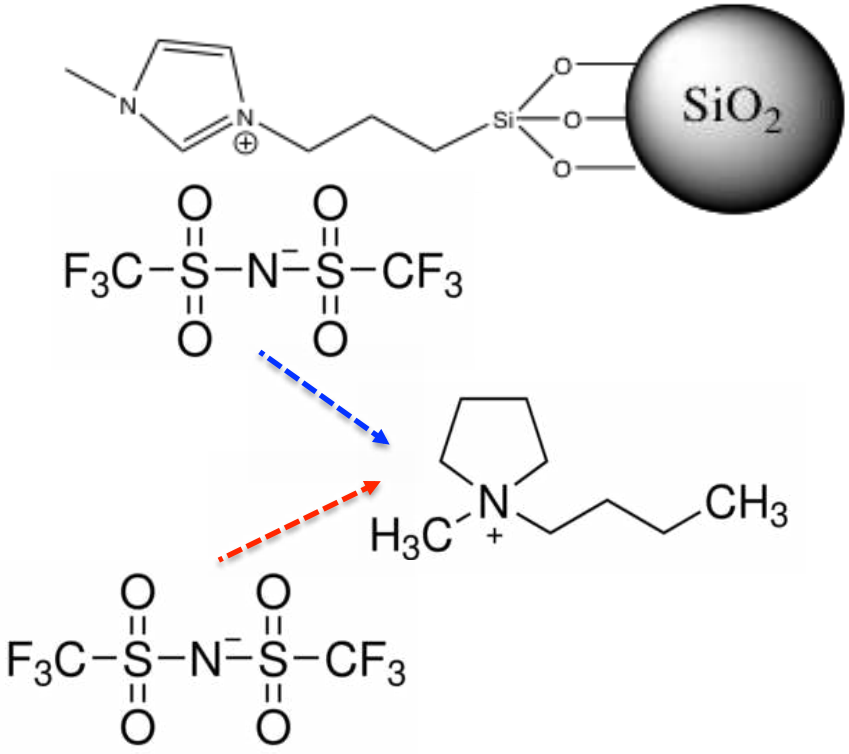

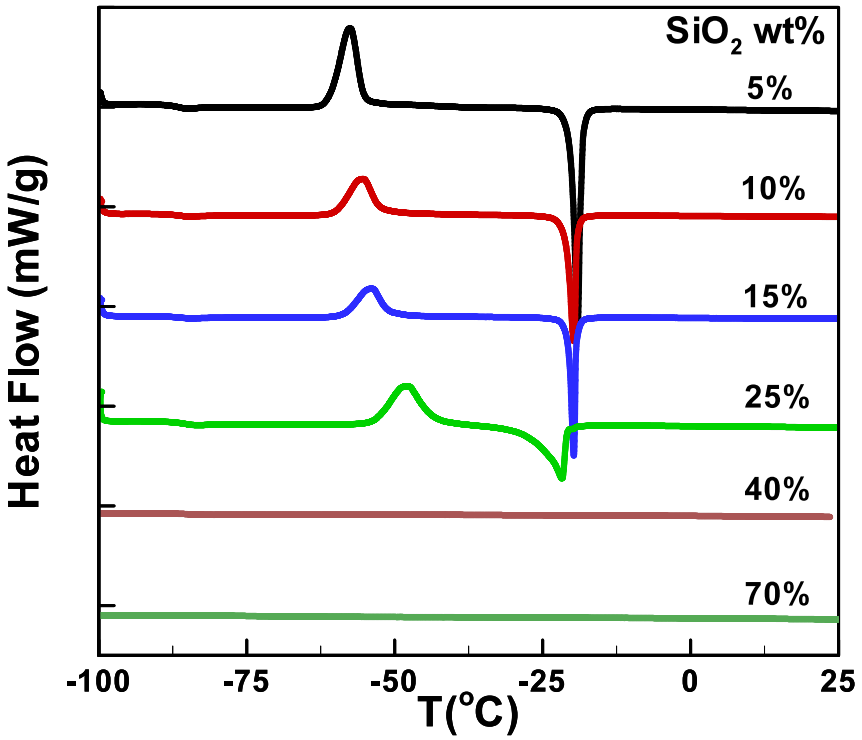

Table of Contents Graphic

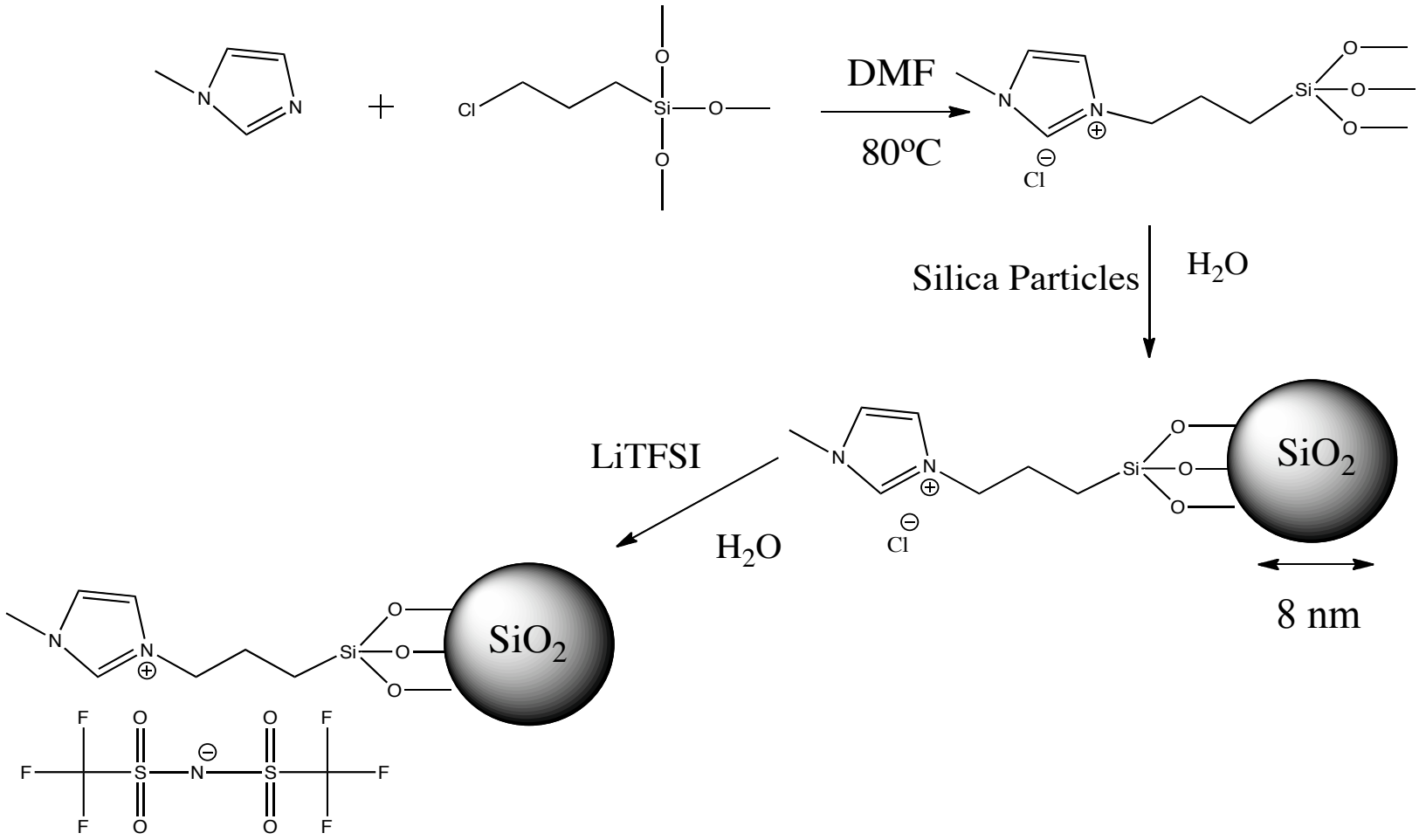

Scheme 1. Procedure for synthesizing SiO_2-BmpyrTFSI nanoparticles.

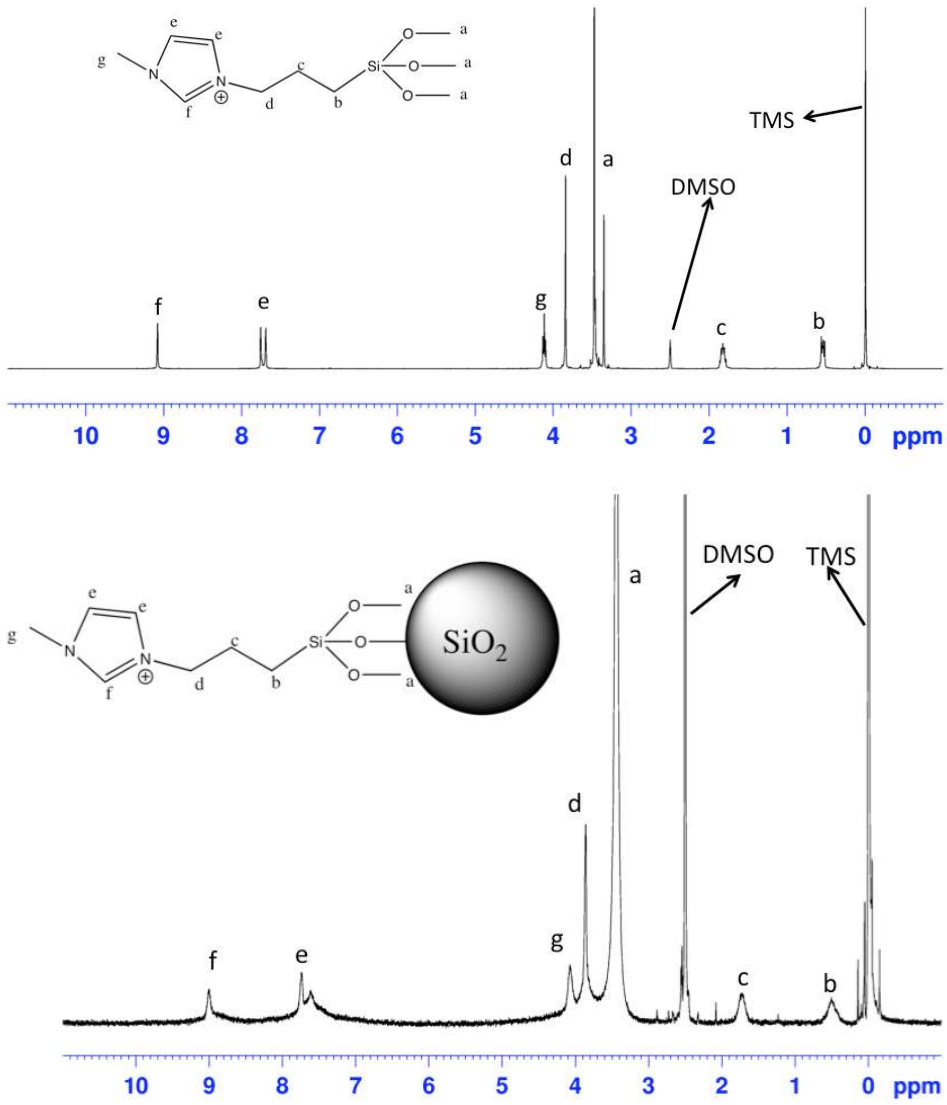
TMS
d
a
DMSO
f
e
g
c
b
10 9 8 7 6 5 4 3 2 1 0 ppm
SiO2
DMSO
TMS
a
d
f
e
g
c
b
10 9 8 7 6 5 4 3 2 1 0 ppm

Figure 1

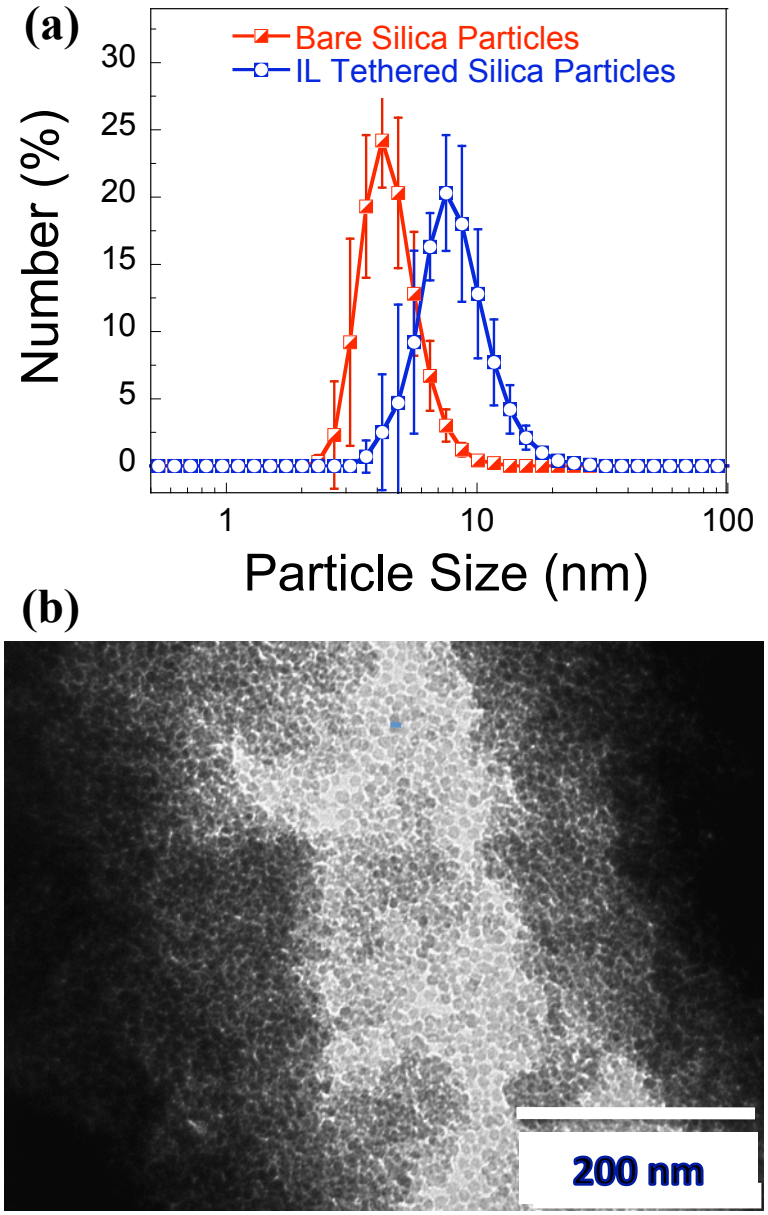
(a)
Bare Silica Particles
IL Tethered Silica Particles
Number (%)
30
25
20
15
10
5
0
1
10
100
Particle Size (nm)
(b)
200 nm

Figure 2

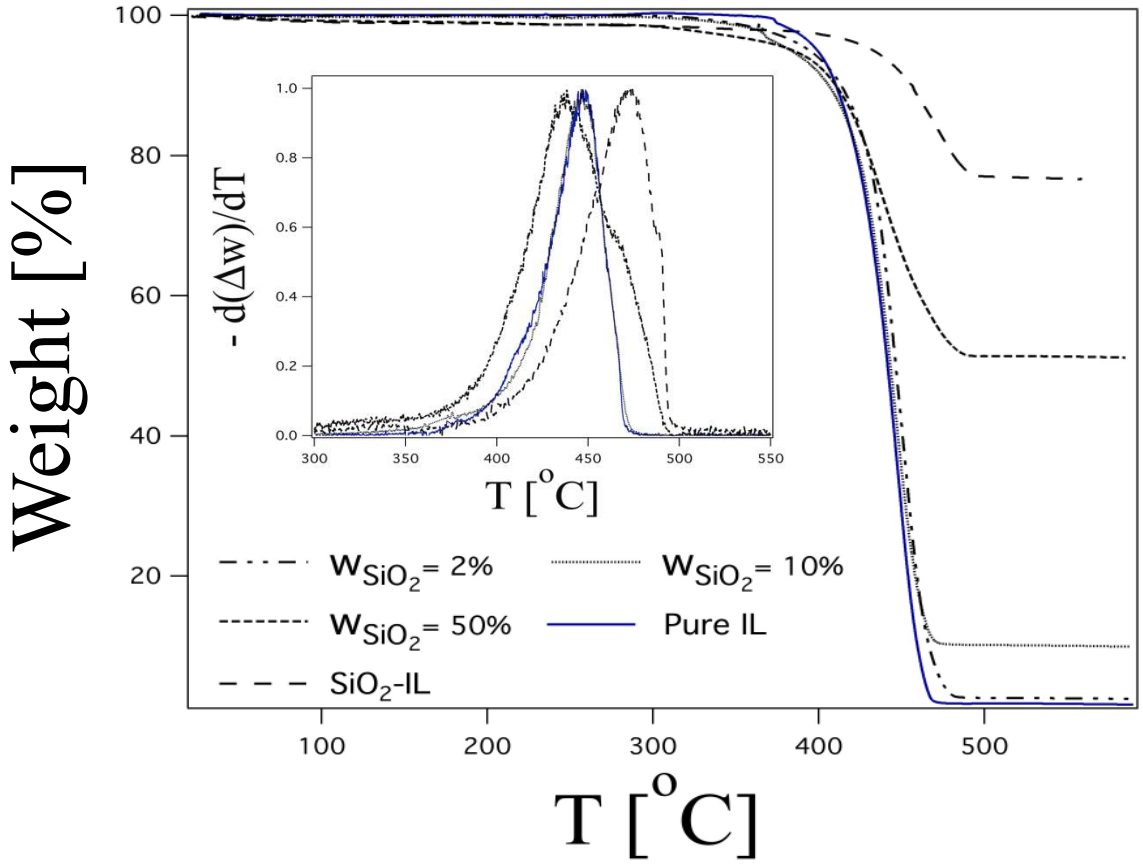
Weight [%]
100
80
60
40
20
100
200
300
400
500
T [°C]
- d(Δw)/dT
1.0
0.8
0.6
0.4
0.2
0.0
300
350
400
450
500
550
T [°C]
W_SiO2 = 2%
W_SiO2 = 10%
W_SiO2 = 50%
Pure IL
SiO2-IL

Figure 3

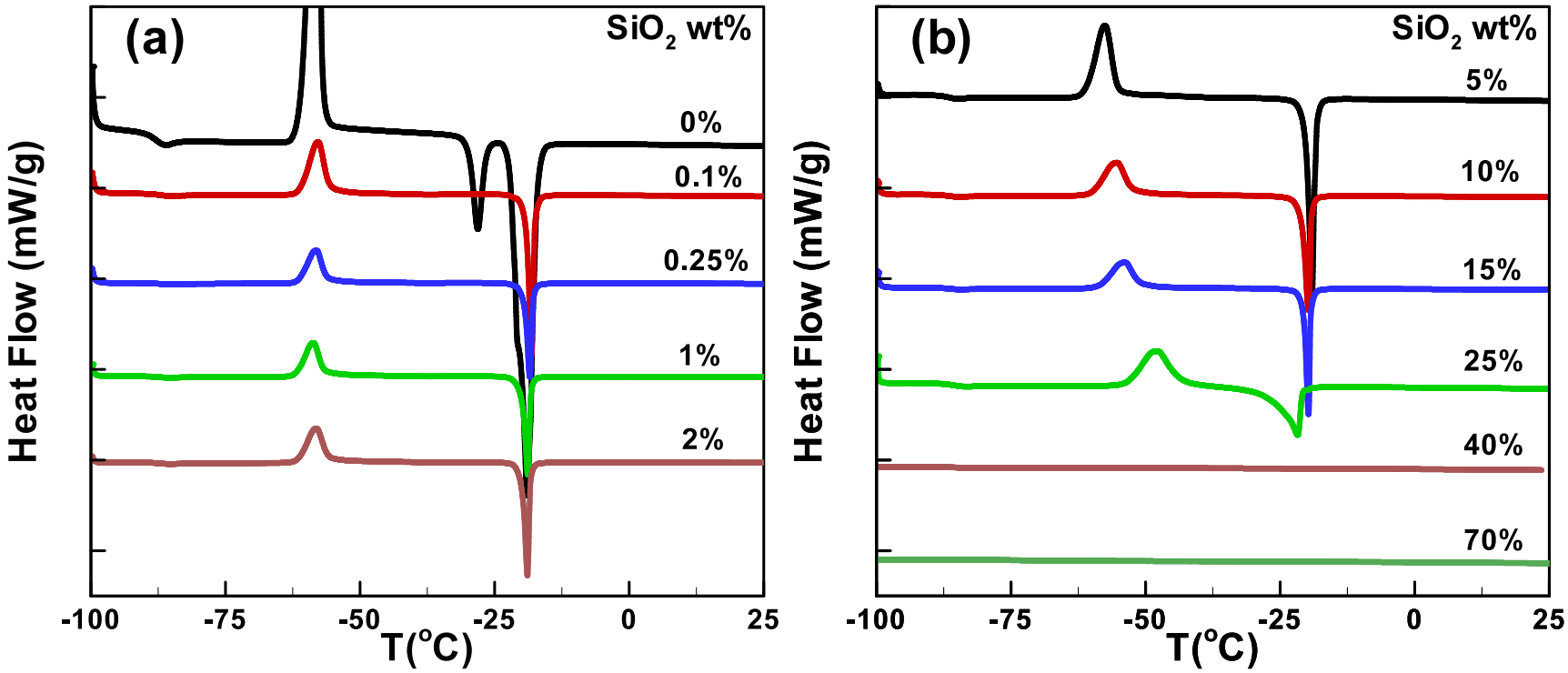
(a)
SiO2 wt%
0%
0.1%
0.25%
1%
2%
Heat Flow (mW/g)
-100
-75
-50
-25
0
25
T(°C)
(b)
SiO2 wt%
5%
10%
15%
25%
40%
70%
Heat Flow (mW/g)
-100
-75
-50
-25
0
25
T(°C)

Figure 4

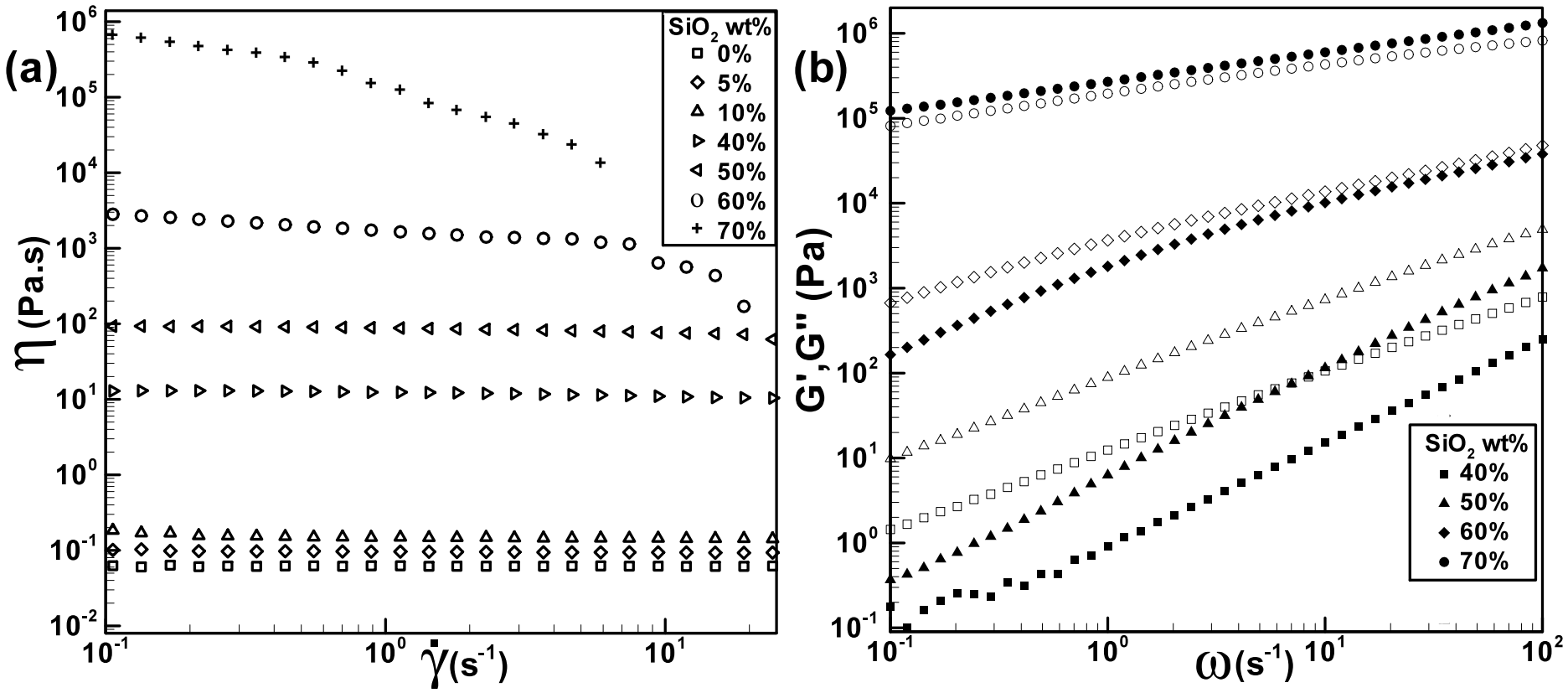

Figure 5

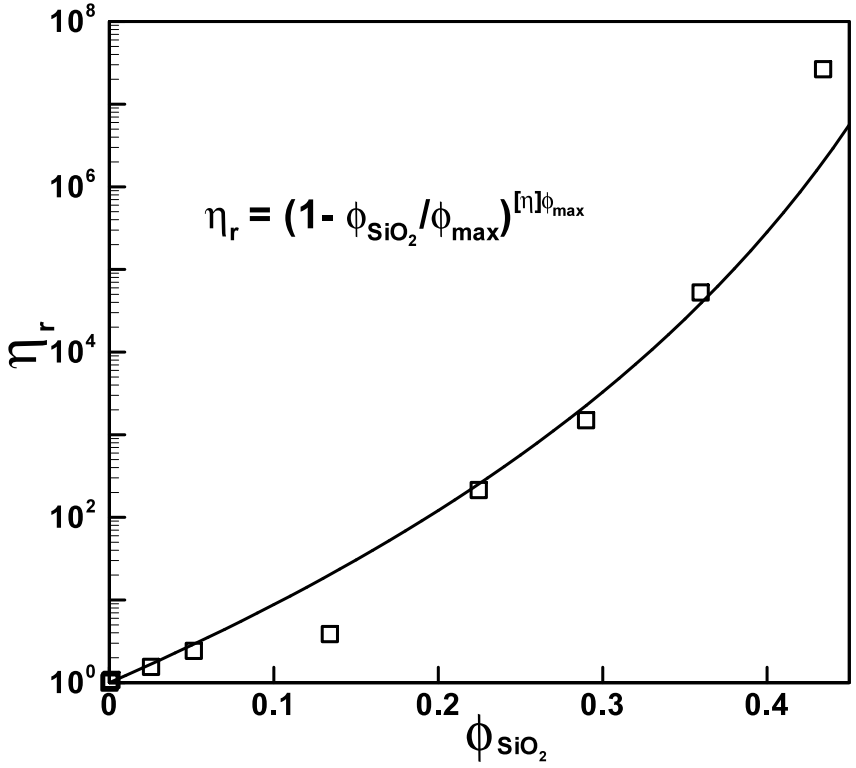
10^8
10^6
10^4
10^2
10^0
η_r
$\eta_r = (1- \phi_{SiO_2}/\phi_{max})^{[\eta]\phi_{max}}$
0
0.1
0.2
0.3
0.4
ϕ_{SiO_2}

Figure 5(c)

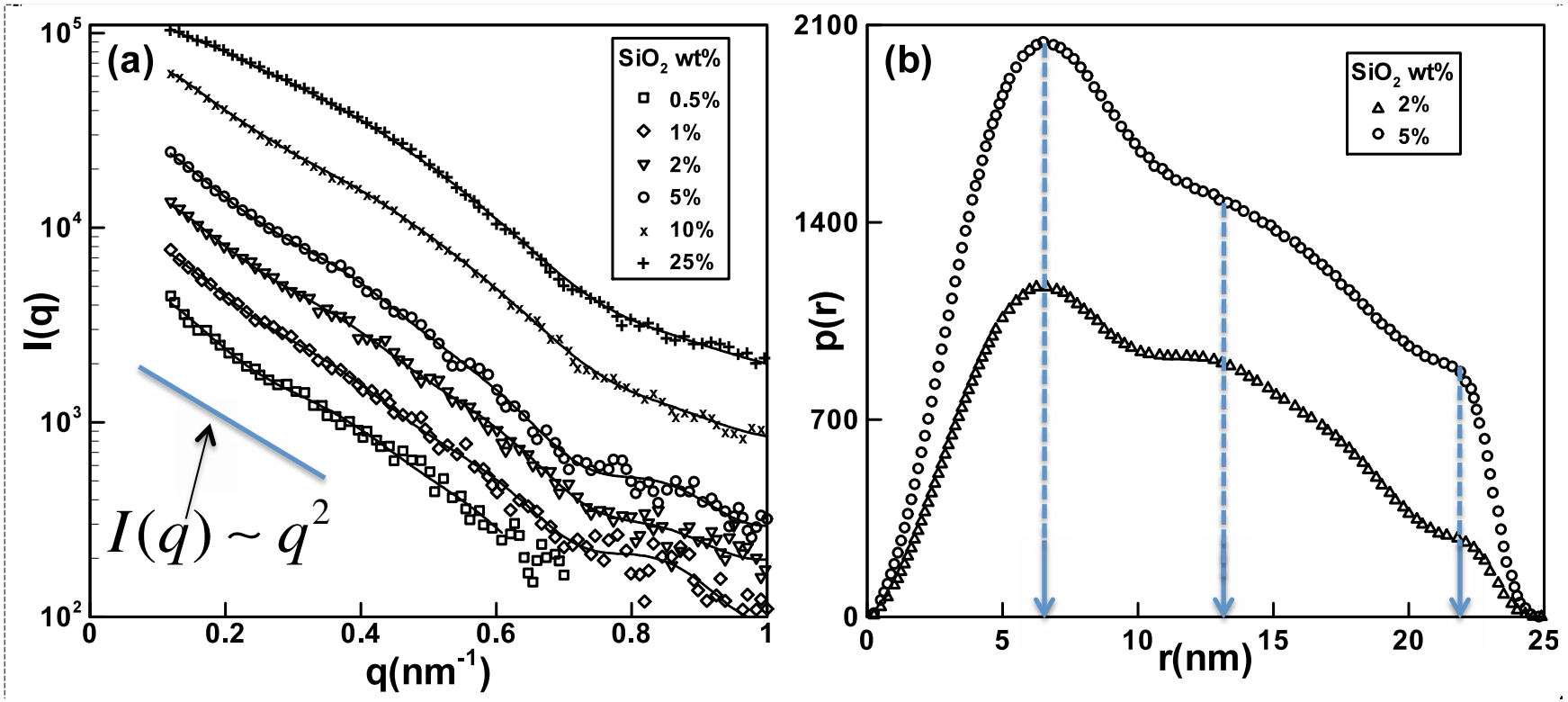

Figure 6